



## Evaluation of the International Vehicle Emission (IVE) model with on-road remote sensing measurements

GUO Hui<sup>1</sup>, ZHANG Qing-yu<sup>1,\*</sup>, SHI Yao<sup>2</sup>, WANG Da-hui<sup>1</sup>

1. Institute of Environmental Engineering, Zhejiang University, Hangzhou 310027, China. E-mail: [hguo1978@yahoo.com.cn](mailto:hguo1978@yahoo.com.cn)

2. Institute of Environmental Science, Zhejiang University, Hangzhou 310027, China

Received 2 August 2006; revised 28 February 2007; accepted 27 March 2007

### Abstract

International Vehicle Emissions (IVE) model funded by U.S. Environmental Protection Agency (USEPA) is designed to estimate emissions from motor vehicles in developing countries. In this study, the IVE model was evaluated by utilizing a dataset available from the remote sensing measurements on a large number of vehicles at five different sites in Hangzhou, China, in 2004 and 2005. Average fuel-based emission factors derived from the remote sensing measurements were compared with corresponding emission factors derived from IVE calculations for urban, hot stabilized condition. The results show a good agreement between the two methods for gasoline passenger cars' HC emission for all IVE subsectors and technology classes. In the case of CO emissions, the modeled results were reasonably good, although systematically underestimate the emissions by almost 12%–50% for different technology classes. However, the model totally overestimated NO<sub>x</sub> emissions. The IVE NO<sub>x</sub> emission factors were 1.5–3.5 times of the remote sensing measured ones. The IVE model was also evaluated for light duty gasoline truck, heavy duty gasoline vehicles and motor cycles. A notable result was observed that the decrease in emissions from technology class State II to State I were overestimated by the IVE model compared to remote sensing measurements for all the three pollutants. Finally, in order to improve emission estimation, the adjusted base emission factors from local studies are strongly recommended to be used in the IVE model.

**Key words:** remote sensing; IVE model; fuel-based emission factor; evaluation

### Introduction

With annual vehicle population growth of above 20% in Chinese large cities in recent years, China faces severer motor vehicle pollutions. The State Environmental Protection Administration of China (SEPA) has identified motor vehicles emissions as the major source of urban air pollution in China (SEPA, 2004). In 2004, on-road vehicles were estimated to contribute over 50% of the nitrogen oxides (NO<sub>x</sub>) to large city's emission inventory (SEPA, 2004). However, since lacking of the resources to develop a comprehensive emission model, emissions from vehicles in China are not well understood and the ability to make accurate future emission estimates does not presently exist. This has limited the ability of decision-makers to design effective control strategies.

The International Vehicle Emissions (IVE) model was developed by the University of California at Riverside, College of Engineering-Center for Environmental Research and Technology, Global Sustainable Systems Research and the International Sustainable Systems Research Center and funded by the U.S. Environmental

Protection Agency (USEPA). It is specifically designed to have the flexibility needed by developing countries in their efforts to address mobile source air emissions, and it has been applied in several cities worldwide including Beijing and Shanghai, China (Nicole *et al.*, 2005; Wang *et al.*, 2006). The advantage of IVE model is that it takes into account the different technologies and conditions that exist in most developing countries and vehicle driving patterns, such as vehicle specific power (VSP) and engine stress distributions which have a profound effect on the tailpipe emissions of vehicles. In order to understand the precision of IVE model in the applications in China and the uncertainties associated with mobile source emission inventories, it needs to evaluate the emission estimates provided by IVE model through comparisons with estimates provided by independent approaches.

On-road optical remote sensing may provide real-world emission factors expressed in grams per liter fuel burnt at a very high level of detail regarding vehicle-specific characteristics such as maker, model year, meteorological conditions, as well as driving conditions (speed and acceleration). In fact, remote sensing has been proposed as an alternative direct method to establish fuel-based mobile source emission inventories in studies conducted in Los Angeles and in the Denver area (Singer *et al.*,

Project supported by the Natural Science Foundation of Zhejiang Province China (No. Y506126). \*Corresponding author.  
E-mail: [qy\\_zhang@zju.edu.cn](mailto:qy_zhang@zju.edu.cn).

2000; Pokharel *et al.*, 2002). And it has been demonstrated that remote sensing may offer many advantages over e.g. tunnel studies for emission model evaluation (Ekström *et al.*, 2004). Therefore, this study carried out an evaluation of the IVE model by utilizing on-road remote sensing measurements conducted on a large number of vehicles for urban, hot stabilized condition in Hangzhou, China.

## 1 Methodology

### 1.1 Remote sensing measurements

All remote sensing measurements were carried out by means of an 4-gas Inspector IV<sup>®</sup> instrument from MD LaserTech Ltd, Tucson, Arizona, which uses tunable diode laser technology to monitor CO and CO<sub>2</sub> emissions, and ultraviolet spectroscopy differential optical absorption spectroscopy technique (UV-DOAS) to measure HC (calibrated as butadiene) and NO.

The remote sensor can directly measure ratios of CO, HC or NO to CO<sub>2</sub>, which are constant for a given exhaust plume and provides emission data as volume% (or ppm by volume) in the undiluted (raw) exhaust. The CO and CO<sub>2</sub> tolerance was 0.25% of concentration or 15% for CO expected concentrations above 3%. In the case of HC, the tolerance was 250 ppm or 15% of the expected HC concentration (whichever was greater) throughout the range of HC concentrations. The NO tolerance was 250 ppm or 15% of the expected NO concentration (whichever is greater) throughout the range of NO concentrations. In order to obtain the best results, the system calibration was carried out once every 2 h. The CO and CO<sub>2</sub> are internally calibrated, and a puff of gas containing certified amounts of 1,3-butadiene and NO is released into the instrument's path and the measured ratios from the instrument are then compared to those certified by the cylinder manufacturer. A device for measuring the speed and acceleration of vehicles driving passing the remote sensor, which includes an emitter bar and a detector bar, was also used.

In this study, the real world on-road petrol vehicle emissions were measured at five sites in Hangzhou during 2004 and early 2005. The locations were selected to measure emissions from a broad range of travel conditions and ages distributed throughout the local area. The relevant important characteristics of each site including the ranges of traffic flow rates, the roads' slope, are described in Table 1. All the five sites were located on streets with slightly uphill geometry, connected to major local arteries in such a way that it was reasonable to expect a negligible share of vehicles operating at cold start enrichment mode. The measurements were carried out during normal working

hours on weekdays. Further details on the remote sensing devices (RSD) and the monitoring campaign have been reported in another paper (Guo *et al.*, 2006).

### 1.2 Calculation of fuel-based emission factors

The remote sensor provides emission data as volume% (or ppm by volume) in the undiluted (raw) exhaust. For the purpose of this study, exhaust concentrations by volume were converted to corresponding fuel-based emission factors expressed as grams of pollutant emitted per liter of fuel burnt. Mass emission factors (EF, g/L) were computed using the following equations:

$$EF_{CO} = \frac{C_{CO}}{C_{CO_2} + C_{CO} + 4C_{HC}} \omega_c \rho_f \frac{M_{CO}}{12} \quad (1)$$

$$EF_{HC} = \frac{C_{HC}}{C_{CO_2} + C_{CO} + 4C_{HC}} \omega_c \rho_f \frac{M_{HC}}{12} \quad (2)$$

$$EF_{NO} = \frac{C_{NO}}{C_{CO_2} + C_{CO} + 4C_{HC}} \omega_c \rho_f \frac{M_{NO}}{12} \quad (3)$$

Where,  $M$  denotes molecular weight,  $\rho_f$  is the density of the fuel (740 g/L for gasoline),  $\omega_c$  is the carbon weight fraction of the fuel ( $\omega_c=0.85$ ) and  $C_{CO}$ ,  $C_{HC}$ , etc. are concentrations given as volume% in the raw exhaust. Since 1,3-butadiene is used to calibrate the instrument, all hydrocarbon measurements reported by the remote sensor are given as 1,3-butadiene equivalents. It is important to note that the remote sensing measurements of HC are based on UV absorption, which only measure aromatics and conjugated alkenes and can not reflect total exhaust HC emissions. Although the particular scale factors for infrared remote sensor have been developed by comparing non-dispersive infrared analyzer measurements with flame ionization detector (FID) measurements (Singer *et al.*, 1998), there is no work conducted to get the scale factors for UV-DOAS to FID measurements yet since UV-DOAS is a new developed technology used in remote sensing. In this study, a substitute method was used to estimate the total exhaust HC emissions from the UV-DOAS based remote sensing. The amount of aromatics and conjugated alkenes in the exhaust HC depends on the fuel composition and driving patterns. The tunnel studies conducted in Chinese major cities in recent years show that on a fleet-average basis, aromatics and conjugated alkenes contribute 24.9%–30.77% of total vehicle exhaust HC emissions in volume concentration (Lu *et al.*, 2003; Wang *et al.*, 2001; Fu *et al.*, 2005). Therefore, the fraction was assumed to be 27.8% in this study. Thus, the HC mass emission factors (EFs) calculated with Eq. (2) were therefore multiplied by a factor of  $3.6 \pm 0.53$ . The HC concentration values were also offset-adjusted in the manner described in Burgard *et al.* (2003). In IVE model, HC emissions are reported

Table 1 Characterization of the five remote sensing measurement sites in Hangzhou

Street name	Street type	Location	Measurement period	Traffic volume (vehicle/h)	Slope (degree)
Dengsheng	City street	North area of Hangzhou City	Apr. and Oct. 2004	284–305	1.5
Zhijiang	Arterial street	South area of Hangzhou City	Feb. 2004	1021–1514	0.7
Fuxing bridge	Overhead road	Central district of Hangzhou City	Nov. 2004, May 2005	667–845	2.2
Meiling	Tunnel	West area of Hangzhou City	Jun. 2005	365–780	1.3
Gudun	City street	West area of Hangzhou City	Aug. 2005	692–941	0

as CH1.85 equivalents whereas the remote sensing instrument reports HC as butadiene equivalents, i.e., CH1.5. Thus, in order to compensate for this, the fuel-specific remote sensing HC emissions were multiplied by a factor MCH1.85/MCH1.5 (i.e. 1.026).

Regarding NO<sub>x</sub>, the remote sensor measures only NO specifically and not NO<sub>2</sub>, whereas the IVE model provides overall NO<sub>x</sub> emissions, expressed as NO<sub>2</sub>. Since NO<sub>2</sub> normally makes up a very small fraction of overall NO<sub>x</sub> in motor vehicle exhaust, in particular for gasoline light-duty vehicles. For instance, tunnel studies have shown that the NO<sub>2</sub> to NO<sub>x</sub> ratio in gasoline motor vehicle exhaust is less than 2%–3% (Kirchstetter *et al.*, 1996; Pierson *et al.*, 1996). Therefore, remote sensor readings for NO, expressed as NO<sub>2</sub> equivalents as common, were set equal to NO<sub>x</sub> emissions in this study.

### 1.3 Calculations with the IVE model

The parameters that affect the hot stabilized emissions from gasoline passenger cars in the IVE model are vehicle fleet technology distribution, vehicle specific power (VSP) and engine stress distribution, inspection and maintenance (I/M) scheme, fuel quality and meteorological condition (humidity and temperature). In the model calculations these parameters were set to values that correspond to the conditions during the remote sensing measurements. Since IVE model shows the results of start-up emissions, hot stabilized emissions and HC evaporative emissions separately, this allows the direct comparison with remote sensing measurements.

VSP is the parameter to characterize the driving patterns specific to the studied area. The equation for determining the instantaneous power of an on-road vehicle is:

$$\text{VSP} = \frac{\text{Power}}{\text{Mass}} \approx 1.1 \times v \times a + 9.81 \times \text{grade} \times v + 0.213 \times v + 0.000305 \times (v + v_w)^2 \times v \quad (4)$$

Where, the VSP is the vehicle specific power (kW/t), the variables  $v$  and  $v_w$  are the vehicle speed and headwind speed (m/s), respectively. The variable  $a$  is the acceleration in m/s<sup>2</sup> and grade is the slope of the roadway (degrees).

The IVE emission factors ( $F_E$ ) (g/km) were also converted into g/L emission factors using the following equation:

$$F_E(\text{g/L}) = F_E(\text{g/km}) \times F(\text{km/L}) \quad (5)$$

Where,  $F_E$  is the pollutant's emission factor and  $F$  is the fuel economy. The average fuel economy for different vehicle types in China is shown in Table 2 (He *et al.*, 2005). The fuel economies for gasoline passenger car (PC) with different cylinder volumes were estimated using the average fuel consumption levels in L/100 km (converted into fuel economy in km/L in this paper) for different vehicle curb weight categories in China (China Automotive Technology and Research Center (CATARC), 2003).

**Table 2 Fuel economy of different vehicle types in China**

Vehicle type	Cylinder volume	Fuel economy (km/L)
Gasoline passenger car (PC)	Average*	11.03
	< 1.5 L	13.60
	1.5–2.0 L	10.33
	>2.0 L	8.45
Light duty gasoline truck (LDGT)	Average*	5.90
Heavy duty gasoline vehicle (HDGV)	Average*	2.84
Motor cycle (MC)	Average*	36.77

\*Reported by He *et al.*, 2005.

### 1.4 Classification of LDGV according to IVE

The IVE model includes a total of 72 different classes of light duty gasoline vehicles (LDGV) including PC and LDGT. A given vehicle belongs to one of the three different “subsectors” depending on the cylinder volume (< 1.5 L, 1.5–3.0 L, and > 3 L), and each subsector contains 22 different “technology classes”. Since there are few PCs belong to the category (cylinder volume > 3 L) in China, the cylinder volumes were divided into three categories: < 1.5 L, 1.5–2.0 L and > 2.0 L in this study. The cylinder volume was directly obtained for PC, on which back the cylinder volume was shown and was captured by the digital camera. The other way is to estimate according to the vehicle weight available from the vehicle register.

The technology class was decided to let the model year govern which technology class that a given car should be assigned to. There are two types of technology classes in the IVE model. One is the vehicle exhaust control technology, while the other is based on the European Standards. The first type was adopted in this study, since the emission factors from technology classes of the first type were derived from real measurements conducted in the U.S. and more accurate than the estimated ones of the second type. The emission standards and corresponding control technologies for new registered LDGV in China are shown in Table 3.

One technology class includes three vehicle use categories in IVE model: < 79000 km, 80000–161000 km and > 161000 km. Since the vehicle use data are not available in the I/M database, they were estimated from the database available in our survey. The survey was conducted for a month in 2004 in all the six I/M stations in Hangzhou City. Approximately 3700 gasoline passenger cars and 1300 gasoline light duty trucks were investigated. The mileage accumulation rate as a function of vehicle age were developed for the two vehicle types (Fig.1) and the vehicle use can be estimated by vehicle age in this study.

### 1.5 Uncertainty analysis and error propagation

Uncertainty and variability in the fuel-based  $F_E$  were quantified by bootstrap simulation. An important advantage of the bootstrap simulation is that no restrictive assumption is required regarding normal distribution. Thus, it can be used on a wide variety of problems. The uncertainty propagation was conducted by Monte Carlo simulation to quantify the uncertainties of emission inventories based on the remote sensing measurements.

**Table 3 Translation between model year and IVE technology class for Chinese vehicles**

Implementation date	Emission standards	Model year	Corresponding technology
January 1, 1993	Conventional (ECE15/03)	1992–1999	Carburetor, non-catalyst/SPFI, open loop non-catalyst
January 1, 2000	State I (Euro I)	2000–2003	SPFI, close loop, 3way/2way catalyst
July 1, 2004	State II (Euro II)	2004–2005	MPFI close loop, 3way catalyst

SPFI: Single point fuel injection; MPFI: multi-point fuel injection.

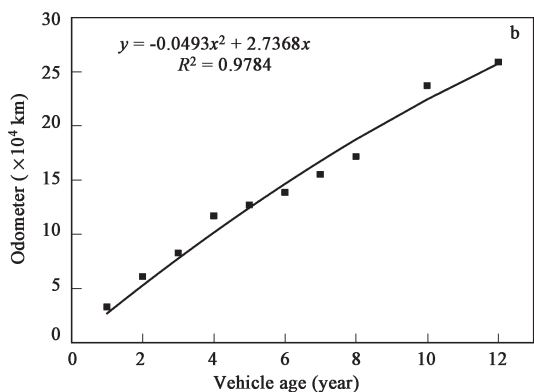
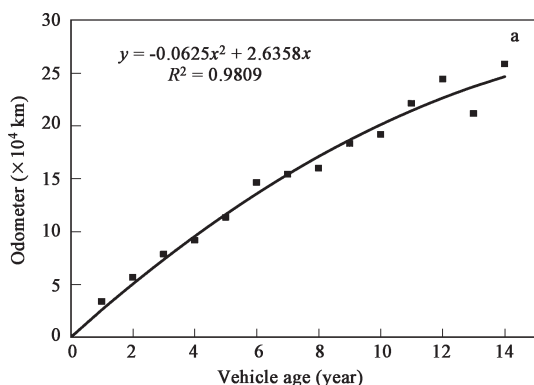


Fig. 1 Vehicle use during the first fourteen years of age. (a) PC; (b) LDGT.

Both simulations were carried out using the commercial software Crystal ball (version 7.2).

## 2 Results and discussion

In total, 59185 measurements were detected during the sampling periods at the 5 sites, of which 46753 (78%) records were valid for CO and CO<sub>2</sub> emissions. Of all the valid measurements, 32260 can be matched to the vehicle registration records, which were retrieved from I/M database for year 2004 and 2005 in Hangzhou provided by Department of Hangzhou Vehicle Emission Administration. Unreadable license plates and many out of city vehicles were the predominant reasons for unmatched licenses.

After assigning subsector and technology classes to the vehicles in the remote sensing data, there were, for gasoline passenger cars, in all, approximately 27000 records with valid CO and HC readings and 24000 records with valid NO readings that could be used for the IVE model evaluation. 18000 valid records were omitted from the analysis because the subsector of these vehicles could not be determined from the available vehicle register data.

Approximately 2500 records with valid CO and HC and 2000 records of valid NO readings for LDGT were also available for the evaluation.

Speed, acceleration and VSP distributions of vehicles recorded with the RSD are shown in Fig.2. These results indicate that vehicles were driven in average at an acceleration of 0.31 km/(h-s), about 56% of the vehicles were driven in an acceleration mode, about 10% in a deceleration mode, and about 34% were in cruising mode. Average speed and VSP were 40 km/h and 6.5 kW/t, respectively. And the VSP distribution shows that most

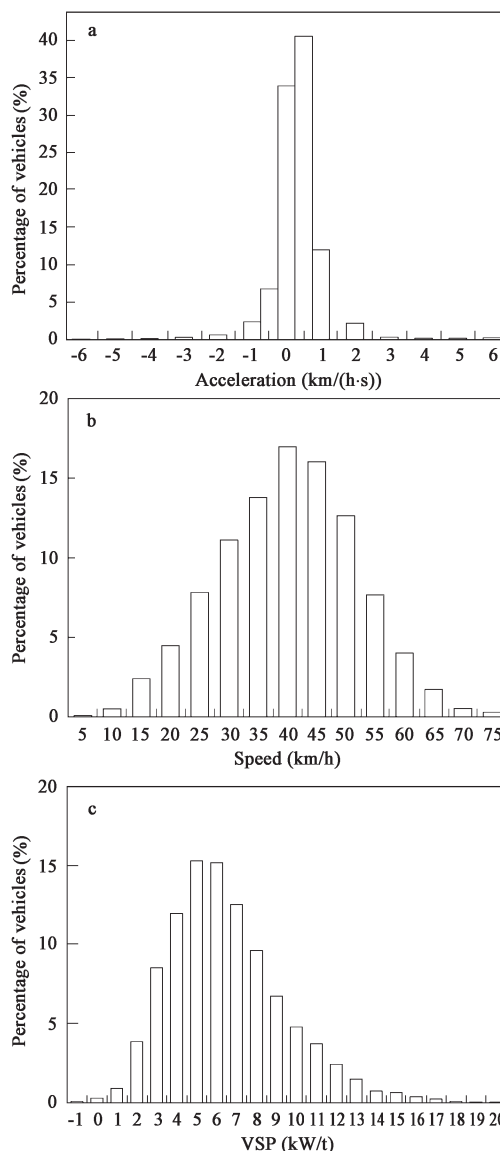


Fig. 2 Speed, acceleration and VSP distributions of vehicles recorded with the RSD. (a) acceleration; (b) speed; (c) VSP.

vehicles measured by RSD operated under positive load, but not under commanded enrichment, which may cause higher emissions (Jiménez-Palacios, 1999), since few VSP about 20 kW/t were observed.

## 2.1 Comparison of CO, NO<sub>x</sub> and HC emission factors of PC

The results from both the IVE model and the remote sensing measurements for gasoline passenger cars are presented in Table 4. Remote sensing studies conducted in Hangzhou shows that CO, HC and NO emissions follow a gamma statistical distribution function (Guo *et al.*, 2007). Thus emission data in each subsector and technology class were gamma distribution fitted and the uncertainty was given as 95% confidence interval of the mean.

Due to the fact that the individual variation between vehicles in terms of on-road emissions may be very significant even if the vehicles belong to the same subsector and technology class, representative average emission factors derived from the remote sensing measurements need to be based on a sufficient number of vehicles. As a rule of thumb, an average emission factor derived from remote sensing needs to be based on measurements on at least 100 vehicles, in order to be considered representative.

For some of the technology classes in Table 4, the same tendency in the discrepancy between model and measurements applied to all the three subsectors and thus warrant further attention. For CO, the remote sensing measurements yielded a little higher emission factors for technology class “conventional” and State I, whereas for technology class State II differences between model and measurements were significantly higher, except for the cylinder less than 1.5. In the case of HC, good agreement

between model and real-world measurements was shown for almost all subsectors and technology classes with no systematic discrepancy observed. Considering NO<sub>x</sub>, the general tendency was that the remote sensing emission factors were much lower than the IVE model emission factors for all the three subsectors, especially for technology class “conventional”. The correlation coefficients ( $r^2$  values) between the IVE and remote sensing emission factors presented in Table 4 were 0.90, 0.81 and 0.95 for CO, NO<sub>x</sub> and HC, respectively. Using the number of cars recorded by remote sensing device in each subsector (Table 4) as weights, average emission factors per technology class were calculated and are presented in Fig.3. The aforementioned tendencies for CO and NO<sub>x</sub> are also evident in Fig.3, whereas in the case of HC, there is a good agreement between the IVE and the remote sensing measurements. For CO, the IVE model calculated emission factors are consistently lower than the emission factors measured from remote sensing for all technology classes. It should be noticed that for technology class State II, IVE model yielded significantly lower CO emission factors than the remote sensing measurements which indicated that IVE underestimated CO emissions from newer vehicles. For NO<sub>x</sub>, however, the IVE model calculated emission factors are consistently higher than the emission factors measured from remote sensing for all technology classes. And the reductions from State II to State I were overestimated by the IVE model.

The first possible source of deviation arises in the default base EFs used in the IVE model estimation, since all the other parameters that affect the hot stabilized emissions in the IVE model were set according to the conditions during the remote sensing measurements, which include

**Table 4 Comparison of hot emission factors for PC according to the IVE model and derived from the remote sensing measurements**

Pollutants	Engine type	Technology class/model year*	No. of PC remote sensing	IVE (g/L)	Remote sensing (g/L)
CO	< 1.5 L	Conventional (1992–1999)	858	352.50	300.75±39.35
		State I (2000–2003)	2718	125.94	230.32±20.11
		State II (2004–2005)	2646	71.26	104.73±24.51
	1.5–2.0 L	Conventional (1992–1999)	1368	290.40	328.73±23.11
		State I (2000–2003)	7984	167.00	245.51±9.56
		State II (04–05)	9036	38.40	116.80±5.82
	> 2.0 L	Conventional (1992–1999)	196	261.82	302.51±68.03
		State I (2000–2003)	1080	172.90	224.96±27.95
		State II (2004–2005)	768	33.70	61.01±11.77
HC	< 1.5 L	Conventional (1992–1999)	858	29.63	27.50±8.27
		State I (2000–2003)	2718	11.87	14.45±4.87
		State II (2004–2005)	2646	2.58	3.54±0.91
	1.5–2.0 L	Conventional (1992–1999)	1368	22.67	28.12±6.48
		State I (2000–2003)	7984	11.30	8.39±1.95
		State II (2004–2005)	9036	2.20	3.61±0.64
	> 2.0 L	Conventional (1992–1999)	196	25.06	24.37±5.17
		State I (2000–2003)	1080	11.21	11.64±1.96
		State II (2004–2005)	768	1.92	2.03±0.73
NO <sub>x</sub>	< 1.5 L	Conventional (1992–1999)	926	24.90	10.02±1.47
		State I (2000–2003)	2724	10.13	7.73±0.31
		State II (2004–2005)	2208	3.52	3.79±0.23
	1.5–2.0 L	Conventional (1992–1999)	1386	32.60	8.22±1.16
		State I (2000–2003)	7178	14.20	5.69±0.30
		State II (2004–2005)	7498	6.30	3.78±0.15
	> 2.0 L	Conventional (1992–1999)	194	34.84	9.26±2.22
		State I (2000–2003)	1008	13.97	7.74±1.1
		State II (2004–2005)	670	5.64	3.87±0.86

\*Model year prior to 1992 have been omitted because of the small number of vehicles in this category from remote sensing.

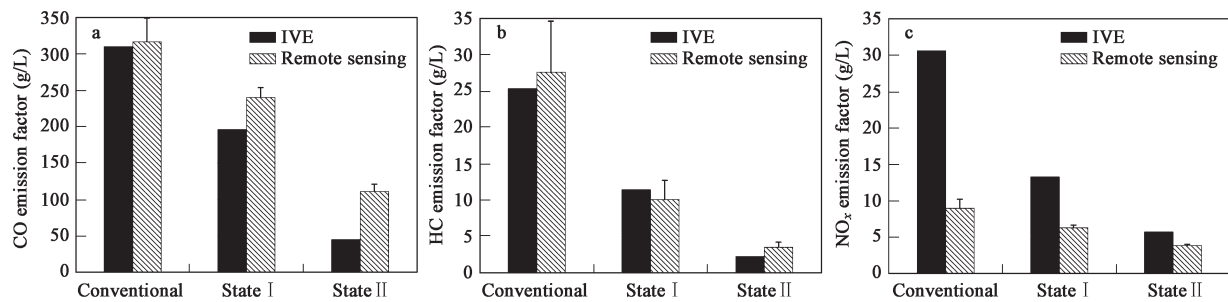


Fig. 3 Comparison of emission factors for gasoline PC as calculated by IVE model and as measured by remote sensing for different technology classes. (a) CO emission factors; (b) HC emission factors; (c) NO<sub>x</sub> emission factors.

vehicle fleet technology distribution, average speed, VSP distribution, I/M scheme, fuel quality and meteorological conditions (humidity and temperature). The default base EFs in IVE model are based on measurements of large amount of vehicles in the United States in Federal Test Procedure (FTP) driving cycle. They were used here because measurement of the base EFs for vehicles belonging to various vehicle types, technologies and vehicle use is not technically or economically feasible in China at this time and also because it is believed that similar technologies should have similar emissions, no matter where they are built or used (Davis, 2005). However, the results showed that there are still some differences between similar technology vehicles used in the U.S. and other countries (especially the developing countries), and this was consistent with the new study conducted by Lents in Mexico City, Sao Paulo and Nairobi (Lents *et al.*, 2005). Thus, the adjusted base emission factors from local studies are strongly recommended to be used in the IVE model to improve the emission estimation.

Another possible source of discrepancy between modeled and measured emission factors results from the influence of vehicle operation under fuel-rich conditions. Emissions associated with enrichment may be included to some extent in the present study because considerable vehicles measured in Hangzhou were likely operating under fuel-rich conditions. According to Heywood (1988), lower level of NO<sub>x</sub> (mainly NO and a smaller proportion of NO<sub>2</sub>) emissions is associated with rich fuel/air stoichiometric by

a lack of excess oxygen, when CO emission is peak caused solely by a lack of adequate air for complete combustion. However, enrichment is not included in the IVE model estimates. This may explain the systematic differences observed between the remote sensing measurements and the IVE model for CO and NO<sub>x</sub>, to some extent.

In addition, the significant discrepancy for conventional technology for NO<sub>x</sub> is likely due to the tendency for older vehicles to lose compression and be operated under fuel-rich conditions, and both factors resulted in lower NO emissions.

## 2.2 Comparison of CO, NO<sub>x</sub> and HC emission factors of other gasoline vehicles

In the present study, the remote sensing measurements included data on approximately 2550 LDGT, 530 HDGV and 250 MC to make comparison with emission factors derived from the IVE model. Since these were small numbers compared to PC, only different technology classes were analyzed for LDGT without considering the cylinder volume (or vehicle weight). In addition, no subsectors and technology classes were divided for HDGV and MC, for insufficient number of measurements.

The results for LDGT, HDGV and MC are presented in Table 5. The IVE emission factors were calculated as an average of the emission factors for different subsectors (three different vehicle weight classes), using the vehicle accounts for each of the subsectors as weights. For LDGT, the general impression is that remote sensing data and IVE

Table 5 Comparison of hot emission factors for LDGT, HDGV and MC according to the IVE model and derived from the remote sensing measurements

Vehicle type	Pollutants	Technology class/model year*	No. of LDGT, remote sensing	IVE (g/L)	Remote sensing (g/L)
LDGT	CO	Conventional (1992–1999)	1016	183.43	280.09±26.50
		State I (2000–2003)	1078	130.00	214.00±29.34
		State II (2004–2005)	460	49.80	164.00±33.00
	HC	Conventional (1992–1999)	1016	13.04	22.01±7.18
		State I (2000–2003)	1078	7.85	13.46±3.13
		State II (2004–2005)	460	1.30	6.64±1.84
	NO <sub>x</sub>	Conventional (1992–1999)	798	24.54	9.39±1.20
		State I (2000–2003)	812	6.84	5.06±0.75
		State II (2004–2005)	384	4.02	3.79±0.93
HDGV	CO	Total	531	186.16	242.90±58.40
	HC	Total	531	14.11	14.22±2.82
	NO <sub>x</sub>	Total	381	13.32	4.24±1.07
MC	CO	Total	249	243.05	301.90±42.48
	HC	Total	249	43.47	24.76±6.11
	NO <sub>x</sub>	Total	222	3.48	4.08±0.98

\*Model year prior to 1992 have been omitted because of the small number of vehicles in this category from remote sensing.

model agree well as regards HC emission factors. However, the technology class State II is an exception, which is different from the PC's situation. Considering NO<sub>x</sub>, good agreement between State I and State II technology was observed, although the emission factor calculated by IVE model was still significantly higher than measured one for conventional technology class. For CO, remote sensing data were still higher than model results. It is important to notice that the reduction of emission factors from State II to State I were overestimated by the IVE model for all the three pollutants.

For HDGV, the model calculated CO emission factors were somewhat lower than measurements, but significantly higher NO<sub>x</sub> were observed. The measured and model calculated HC emission factors show good agreement. In the case of MC, NO<sub>x</sub> were matched well, compared to higher measured CO and somewhat lower measured HC emission factors. Limited by measurement number, these were only rough comparisons conducted for the two vehicle types.

### 2.3 Comparison of overall CO, NO<sub>x</sub> and HC emissions for LDGV

To access the importance of the observed discrepancies in emission factors for different technology classes between the IVE model and the remote sensing measurements, the overall CO, NO<sub>x</sub> and HC emissions for LDGV were estimated. The fuel economy and measurement frequency of different car and truck subgroups were used to calculate relative fuel use by each of these subgroups. Since remote sensing measurements are conducted in real-world traffic with random vehicle samples, the car counts in Tables 3 and 4 represent an activity estimate. Mathematically, the process is given as follow:

$$f_i = \frac{n_i/N/F_i}{\sum (n_i/N/F_i)} \quad (6)$$

where,  $i$  is the technology subgroup,  $n$  is the number of measurements of subgroup,  $N$  is the total number of measurements (including HDGV and MC),  $f_i$  is the relative fuel use of each subgroup,  $F_i$  is the fuel economy. Then the fuel use can be combined with emission factors for each of the subgroups ( $EF_i$ ) and the total fuel consumption ( $V$ ) to obtain an overall emissions of subgroup  $i$ .

$$E_i = EF_i \times f_i \times V \quad (7)$$

**Table 6 Comparison of overall CO, HC and NO<sub>x</sub> emissions for LDGV in Hangzhou in 2005**

Pollutant	Remote sensing inventory (t/a)	IVE inventory (t/a)	Deviation (%)
CO	167845.49±13590.63	105863.78	-36.93
HC	8263.63±2255.09	7275.85	-11.95
NO <sub>x</sub>	4806.08±418.69	10143.13	111.04

the total gasoline sales in Hangzhou metropolitan area in 2005 was approximately 780000 t and among them almost 87% was consumed by the transportation (Hangzhou Development and Reform Commission, 2006). The gasoline density is 740 g/L. Thus the total fuel consumption was  $9.17 \times 10^8$  L. Although some fuel is consumed in the process of vehicle starting and fuel evaporation, it does not contribute appreciably to the inventory since not much fuel is consumed during the short period of time when the vehicle is in "start" mode (Singer *et al.*, 1998; Schifter *et al.*, 2005). Therefore, it was assumed that all fuel was used during stabilized vehicle operations.

The total emission estimates developed from remote sensing in this study and 95% confidence intervals, compared with the IVE estimation, are summarized in Table 6. Table 6 shows that the IVE modeled emission inventory for LDGV are -36.93% lower, -11.95% lower and +111.04% higher, than the inventory based on remote sensing measurements for CO, HC and NO<sub>x</sub>, respectively. The deviations are expressed as percentages of total emissions, as calculated using remote sensing data. Propagation of errors led to overall uncertainties in tons of pollutant per year for CO, HC and NO<sub>x</sub> as 8.1%, 27.3% and 8.7% respectively. This only qualified uncertainty and variability of emission factors from on-road remote sensing and HC scale factor estimation. There are also other uncertainties which are hard to be qualified. One source of these uncertainties may come from fuel economy used in this study. It is known that motor vehicle's fuel economy strongly depends on its driving conditions, however, this can not be considered in the RSD study. In addition, the emission contribution from out-of-city vehicles were not considered in this study for lack of their specific informations.

Fig.4 displays the emission estimates of different technology subgroups for LDGV. For CO, Fig.4 shows that the model underestimates the total emissions for three technology classes. The contributions from State I and State II vehicles to the total discrepancy are almost the same.

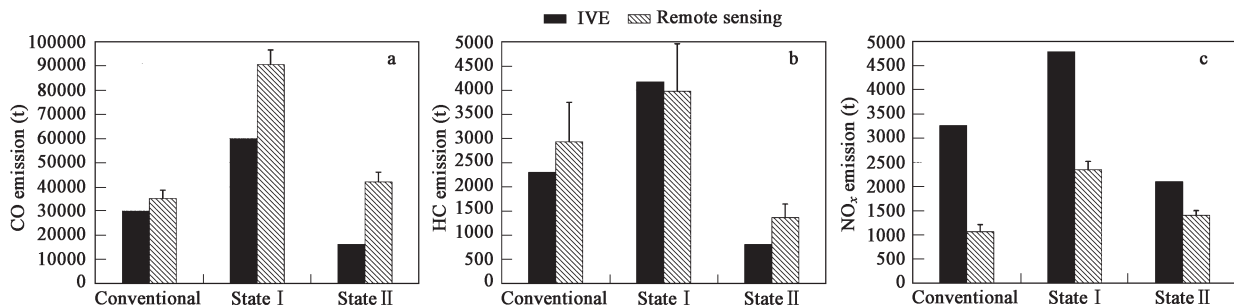


Fig. 4 Calculated emissions for LDGV driving under hot stabilized conditions in urban areas in Hangzhou in 2005 versus technology class. (a) CO emissions; (b) HC emissions; (c) NO<sub>x</sub> emissions.

Furthermore, as older vehicles belonging to technology class “conventional” are gradually phased out from the vehicle fleet, it seems that the underestimation of total CO emissions for LDGV in IVE model will increase in relative terms. In the case of HC, Fig.4 shows that the agreement between remote sensing and IVE model, which was excellent for overall emissions, is slightly weaker for individual technology class. Even though the discrepancies in HC emissions for individual technology classes are small, the discrepancies observed between the model predictions and the remote sensing data as regards HC emission factors for State II may become increasingly important as these technology classes penetrate the vehicle fleet. Regarding NO<sub>x</sub>, the IVE model over predicts NO<sub>x</sub> emissions for all technology classes. The largest contribution to the total discrepancy comes from State I vehicles.

### 3 Conclusions

For gasoline passenger cars operating under hot stabilized conditions in urban traffic, this study has demonstrated a good agreement between the IVE model and on-road optical remote sensing measurements in the case of HC emissions, a reasonable agreement for CO but a weaker agreement in the case of NO<sub>x</sub> emissions. The overall correlation coefficients,  $r^2$ , between emission factors derived from IVE and from remote sensing were 0.90, 0.95 and 0.81 for CO, HC and NO<sub>x</sub> respectively. The NO<sub>x</sub> emission factors by technology class differed significantly between the remote sensing data and the IVE model with systematically lower emission factors according to the remote sensing measurements. A comparison of HC emission factors for LDGT, demonstrated a reasonable agreement between IVE and the remote sensing data. A notable result was that the decrease in emissions from technology class State II to State I were overestimated by the IVE model compared to remote sensing measurements for all three pollutants.

Calculations of annual emissions of CO, HC and NO<sub>x</sub> for LDGV operating under hot stabilized conditions in urban traffic in metropolitan area of Hangzhou City were performed based on the emission factors derived in the present study and available fuel consumption data. The resulting CO emission using IVE emission factors was 37% lower than that using remote sensing emission factors. For NO<sub>x</sub>, the IVE results were 113% higher. For HC, however, the two methods resulted in almost the same emission.

Finally, this study only conducted evaluation of IVE model by remote sensing data from gasoline vehicle measurements, limited by the remote sensing instrument. Further studies on model evaluation for diesel vehicles especially, for trucks and buses should be conducted to help clearly understand the precision of IVE model in the applications in China and further identify the uncertainties associated with mobile source emission inventories.

### Acknowledgements

This work was supported grant number M203102 from

the Natural Science Foundation of Zhejiang Province, China. Its contents are solely the responsibility of the authors and do not necessarily represent official views of the funding agency. The authors would like to thank Hangzhou Vehicle Emission Administration and Hangzhou Vehicle Management Bureau for offering the specific vehicle information data.

### References

- Burgard D A, Bishop G A, Williams M J *et al.*, 2003. On-road remote sensing of automobile emissions in the Denver area: Year 4, January 2003[EB]. <http://www.feat.biochem.du.edu/reports.html>.
- CATARC (China Automotive Technology and Research Center), 2003. Study of fuel economy legislation and policy in China (EB). [http://www.efchina.org/documents/Fuel\\_Economy\\_CN.pdf](http://www.efchina.org/documents/Fuel_Economy_CN.pdf).
- Davis N C, Lents J M, Osses M *et al.*, 2005. Development and application of an International Vehicle Emissions Model[C]. Transportation Research Board 81st Annual Meeting. Washington.
- Ekström M, Sjödin Å, Andreasson K, 2004. Evaluation of the COPERT III emission model with on-road optical remote sensing measurements[J]. *Atmospheric Environment*, 38: 6631–6641.
- Fu L L, Shao M, Liu Y *et al.*, 2005. Tunnel experimental study on the emission factors of volatile organic compounds (VOCs) from vehicles[J]. *Acta Scientiae Circumstantiae*, 25(7): 879–885.
- Guo H, Zhang Q Y, Yao S *et al.*, 2006. Characterization of on-road CO, HC and NO emissions for petrol vehicle fleet in China city[J]. *Journal of Zhejiang University, SCIENCE/B* (7): 532–541.
- Guo H, Zhang Q Y, Yao S *et al.*, 2007. On-road remote sensing measurements and fuel-based motor vehicle emission inventory in Hangzhou, China[J]. *Atmospheric Environment*, 41: 3095–3107.
- Hangzhou Development and Reform Commission, 2006. The management of Hangzhou fuel market[EB]. [http://oil-synggs.mofcom.gov.cn/oil/portalManage/wsa\\_display\\_Article.jsp?articleId=0000001d2a0018e7fc61b1&subjectID=0000005d2000fe8fe4d7e5](http://oil-synggs.mofcom.gov.cn/oil/portalManage/wsa_display_Article.jsp?articleId=0000001d2a0018e7fc61b1&subjectID=0000005d2000fe8fe4d7e5).
- He K B, Huo H, Zhang Q *et al.*, 2005. Oil consumption and CO<sub>2</sub> emissions in China's road transport: current status, future trends, and policy implications[J]. *Energy Policy*, 33: 1499–1507.
- Heywood J B, 1988. *Internal combustion engine fundamentals*[M]. New York: McGraw-Hill. 352–480.
- Jiménez-Palacios J L, 1999. Understanding and quantifying motor vehicle emissions with vehicle specific power and TILDAS remote sensing[D]. Ph. D Thesis. Massachusetts Institute of Technology.
- Kirchstetter T, Harley R A, Littlejohn D, 1996. Measurement of nitrous acid in motor vehicle exhaust[J]. *Environmental Science and Technology*, 30: 2843–2849.
- Lents J M, Davis N C, Osses M *et al.*, 2005. Measurement of in-use passenger vehicle emissions in three urban areas of developing nations[EB]. [2005-11-25]. <http://www.gssr.net/ive/index.html>.
- Lu S H, Bai Y H, Chen Y K *et al.*, 2003. The characteristics of volatile organic compounds (VOCs) emitted from motor vehicle in Beijing[J]. *China Environmental Science*, 23(2):

- 127–130.
- Nicole D, James L, Mauricio O *et al.*, 2005. Transportation research board 81st annual meeting[C]. Washington D.C., Jan, 2005.
- Pierson W R, Gertler A W, Robinson N F *et al.*, 1996. Real-world automotive emissions-summary of studies in the Fort McHenry and Tuscarora mountain tunnels[J]. *Atmospheric Environment*, 30: 2233–2256.
- Pokharel S S, Bishop G A, Stedman D H, 2002. An on-road motor vehicle emissions inventory for Denver: an efficient alternative to modeling[J]. *Atmospheric Environment*. 36: 5177–5184.
- Schifter I, Dłaz L, Mgica V *et al.*, 2005. Fuel-based motor vehicle emission inventory for the metropolitan area of Mexico City[J]. *Atmospheric Environment*, 39: 931–940.
- SEPA (State Environmental Protection Administration of China), 2004. 2004 Annual Plenary Meeting of Joint Research Network on Vehicle Emission Control Technologies[R].
- Singer B C, Harley R A, Littlejohn D *et al.*, 1998. Scaling of infrared remote sensor hydrocarbon measurements for motor vehicle emission inventory calculations[J]. *Environmental Science and Technology*, 31: 927–931.
- Singer B C, Harley R A, 2000. A fuel-based inventory of motor vehicle exhaust emissions in the Los Angeles area during summer 1997[J]. *Atmospheric Environment*, 34: 1783–1795.
- Wang W, Liang B S, Zeng F G *et al.*, 2001. Study on pollution characteristics and emission factors of volatile organic compounds in Tanyugou highway tunnel[J]. *Research of Environmental Sciences*, 14(4): 9–12.
- Wang H K, Chen C H, Huang C *et al.*, 2006. Application of the International Vehicle Emission model for estimating of vehicle emissions in Shanghai[J]. *Acta Scientiae Circumstantiae*, 26(1): 1–9.